
**1. Dynamin-I Inhibitors from Sessile
Marine Invertebrates;
2. Chemotaxonomy of *Cystophora* spp.**

Doctor of Philosophy (Chemistry)

Ian P. Holland

B. Sc. (Hons)

School of Environmental and Life Sciences
(Faculty of Science and Information Technology)

University of Newcastle, Australia

July, 2011



International Year of
CHEMISTRY
2011

Declaration

This thesis contains no material which has been accepted for the award of any other degree or diploma in any university or other tertiary institution and, to the best of my knowledge and belief, contains no material previously published or written by another person, except where due reference has been made in the text. I give consent to this copy of my thesis, when deposited in the University Library, being made available for loan and photocopying subject to the provisions of the Copyright Act 1968.

.....
Ian P. Holland

July, 2011

~ Somewhere, something incredible is waiting to be known ~

Dr. Carl E. Sagan, 1934–1996

Acknowledgements

First and foremost, I would like to express my unconditional gratitude to both of my supervisors, Prof. Adam McCluskey and Dr. Ian van Altena, both of whom have encouraged and inspired me throughout my PhD. For the guidance, instruction, and friendship you have both given me I am immeasurably grateful.

I would like to thank the past and present members of the Marine Natural Products group at the University of Newcastle, in particular Kate Wright and Mohammed Ghandourah for their assistance with sample collections, Dr. Kongkiat Trissuwan for his assistance with the isolation of compounds from *C. torulosa* and Diana Zaleta-Pinet and Yuhanis Mhd Bakri for their enduring help and advice.

I would like to thank Ass. Prof. Phil Robinson and all of the members of the Cell Signaling group at the Children's Medical Research Institute (Westmead, NSW, Australia). In particular I would like to pay a special thanks to Ngoc Chau and Annie Quan for their advice and guidance while running the dynamin-I assay.

I am grateful to Dr. Merrick Ekins (The Queensland Museum, South Brisbane, QLD, Australia) for sponge identification, Cherie Motti (The Australian Institute of Marine Science, Townsville, QLD, Australia) for high resolution mass spectrometry and Jennette Sakoff and Jayne Gilbert for the anticancer assays. I would also like to acknowledge Dr. Monica Rossignoli for her patience and assistance in NMR and GC-MS troubleshooting.

I would like to thank all of my friends at the University of Newcastle, in particular Ryan Shaw and John Tulloch. For your advice, support and friendship I am truly grateful.

Last, but not least, I would like to thank my parents, Bob and Coleen, and brother, Mark. Without their ongoing support and encouragement I know I would not have made it this far.

To my parents, Bob and Coleen

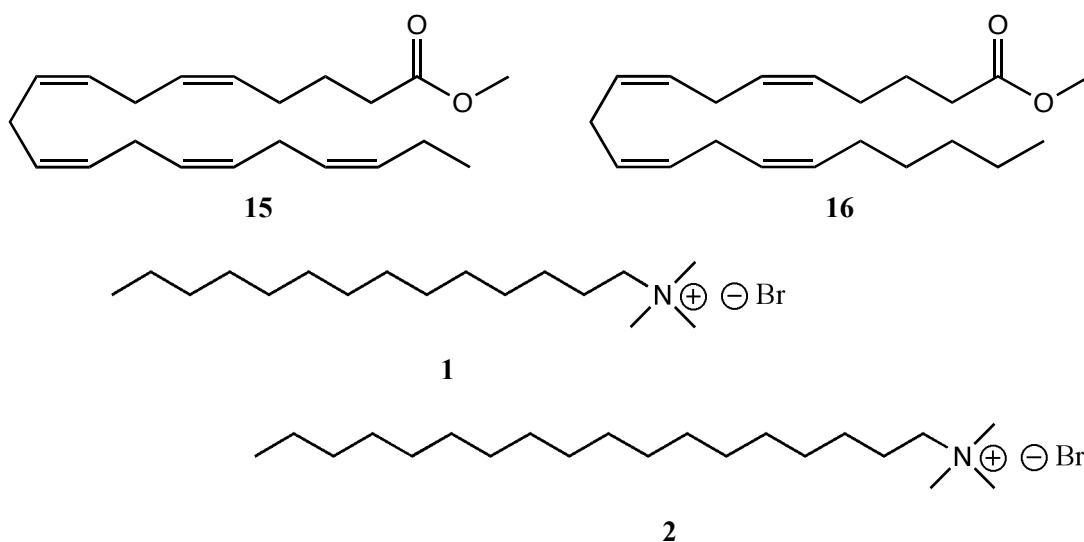
Abbreviations and Symbols

1D	One-dimensional
2D	Two-dimensional
Å	Angstroms
APCI	Atmospheric pressure chemical ionisation
ax	Axial
$[\alpha]_D$	Specific optical rotation
<i>br</i>	broad (in NMR)
BuOH	Butanol
^{13}C NMR	Carbon nuclear magnetic resonance (spectroscopy)
$\text{C}_5\text{D}_5\text{N}$	Deuterated pyridine
C_6D_6	Deuterated benzene
CDCl_3	Deuterated chloroform
CHCl_3	Chloroform
CH_2Cl_2	Dichloromethane
CMT	Charcot-Marie-Tooth
CNM	Centronuclear myopathy
COSY	Correlation spectroscopy
δ	Chemical shift in ppm
DEPT	Distortionless enhancement by polarization transfer
DHA	Docosahexanoic acid
ϕ	Dihedral angle
EI	Electron impact
EPA	Eicosapentaenoic acid
eq	Equatorial
EtOAc	Ethyl acetate
ESI	Electrospray ionisation
FT	Fourier transform
GC	Gas chromatography
GI	Growth Inhibition

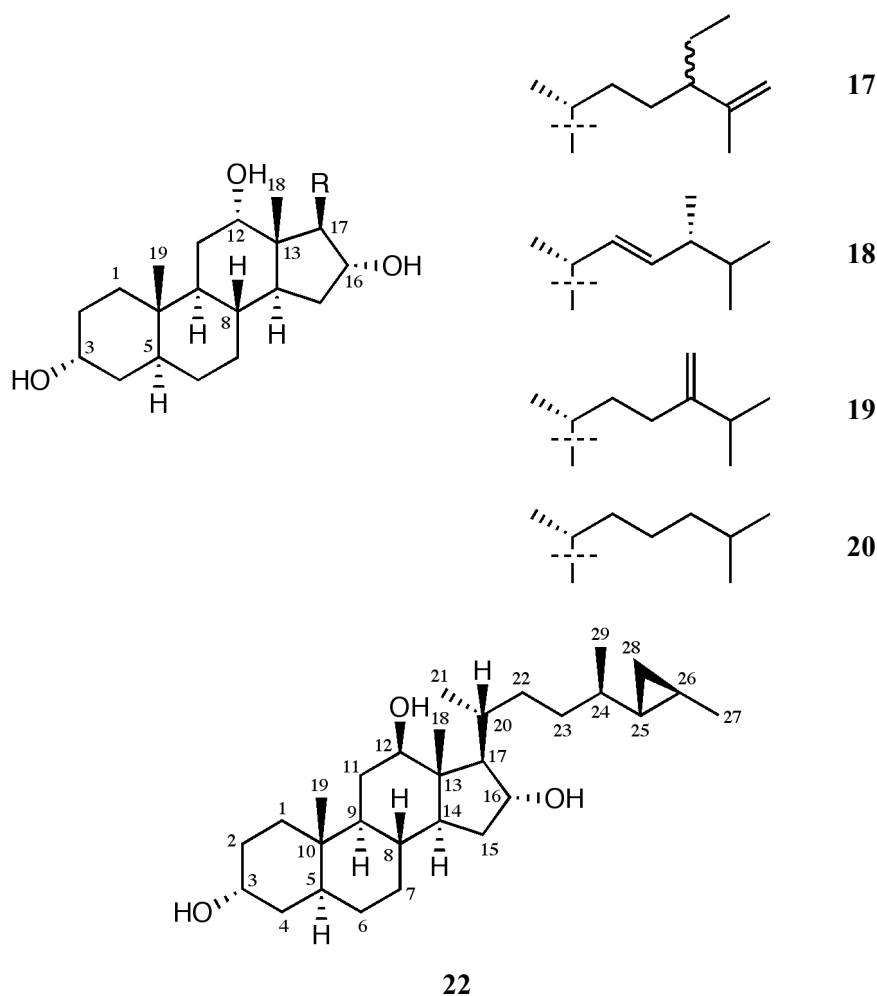
^1H NMR	Proton nuclear magnetic resonance (spectroscopy)
HMBC	Heteronuclear multiple bond correlation
HMQC	Heteronuclear multiple quantum coherence
HPLC	High performance liquid chromatography
Hz	Hertz
<i>i</i> -octane	2,2,4-trimethylpentane
IC ₅₀	Half Maximal Inhibitory Concentration
IR	Infrared
<i>J</i>	Coupling constant
λ_{max}	Absorbance maximum
LC	Liquid chromatography
MeOD	Deuterated methanol
MeOH	Methanol
MiTMAB	Myristyltrimethylammonium bromide
MS	Mass spectrometry
mult	Multiplicity
<i>m/z</i>	Mass to charge ratio
NMR	Nuclear magnetic resonance
NOE	Nuclear Overhauser enhancement
NOESY	Nuclear Overhauser effect spectroscopy
OctTMAB	Octadecyltrimehtylammonium bromide
Petrol	Light Petroleum (60°C – 80°C fraction)
ppm	Parts per million
PUFA	Polyunsaturated fatty acid
<i>t</i> _R	Retention time
SAR	Structure-activity relationship
Sp.	Species
TLC	Thin-layer chromatography
UV	Ultraviolet

Abstract

A colourimetric GTPase assay was utilised to screen a marine natural products library of extracts with the goal of identifying novel dynamin-I inhibitors. Bioassay-guided fractionation of an active marine sponge (unknown Australian species) fraction led to the isolation of the methyl esters of eicosapentaenoic acid (EPA) (**15**) and Arachidonic acid (**16**). These compounds are structurally similar to the known dynamin-I inhibitors MiTMAB (**1**) and OcTMAB (**2**), however, **15** and **16** were inactive in the dynamin-I GTPase bioassay.

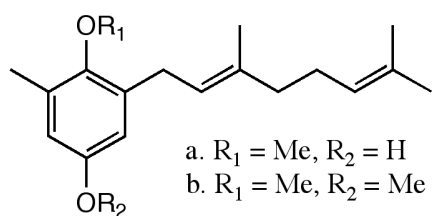


An extract of another Australian marine sponge *Psammocelmma* sp. was found to possess dynamin-I inhibitory activity. Bioassay-guided fractionation led to the isolation of four new trihydroxysterols (**17–20**) related to aragusterol G (**22**). While **17** was inactive in the dynamin-I bioassay, bioassays did reveal that compounds **17–20** inhibited the growth of colorectal, breast, ovarian and prostate cancer cell lines (GI₅₀ 5–27 μM). The additional insight that these new compounds provide to previous SAR studies is also discussed.

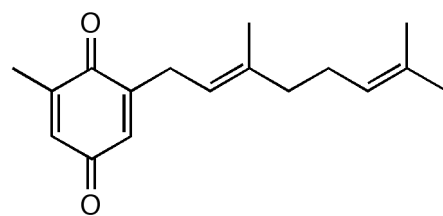


In addition, the chemistry of the brown algae *Cystophora torulosa* and *C. xiphocarpa* were investigated. It is well known that *C. torulosa* produces a range of secondary metabolites including resorcinols, tocotrienols, polyunsaturated alkene chains and phloroglucinols. Considering these are fairly ‘standard’ *Cystophora* compounds that have also been isolated from apparently closely related *Cystophora* species, the isolation of the previously discovered meromonoterpenes **51a**, **52** and **53** was unusual. Since these meroterpenoids potentially could be used as geographic marker compounds for New Zealand populations of *C. torulosa* and suggest an unexpectedly close relationship with *C. harvei* it was judged necessary to confirm the isolation of the meromonoterpenoids from *C. torulosa*. *Cystophora torulosa* was reinvestigated with the aim of re-isolating **51a**, **52** and **53**. This investigation yielded many of the known *C. torulosa* compounds including polyenes (**40** and **41**), an isoprenyl chroman (**48**), a resorcinol (**42**) and fucosterol (**92**) but not the meromonoterpenes in question. It is apparent

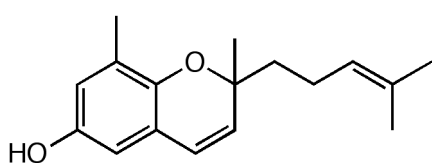
from comparison of the TLC profile of the crude *C. torulosa* extract with the isolated compounds that this investigation has not yet been exhausted and, as such, is ongoing.



51



52



53



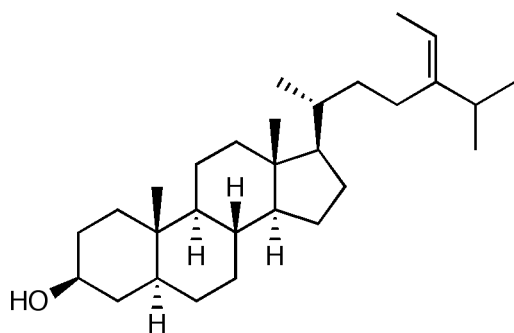
40



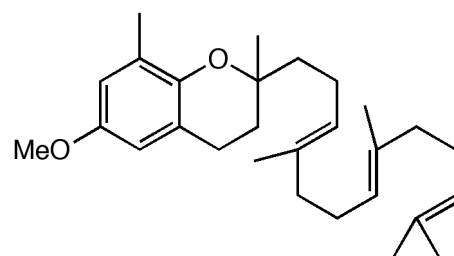
42



41



92



48

As the putative ancestor of the genus, *C. xiphocarpa* was expected to possess only the more common and wide-spread *Cystophora* compounds, such as phloroglucinols and tocotrienols. To date no secondary metabolites are reported from the species and it was decided to investigate the chemistry of specimens collected in Tasmania. GC-MS of the methyl esters of a transesterified triacylglycerol isolated identified at least thirteen acyl chains, 14:0, 16:3 n -6,

16:0, 18:3*n*-6, 18:4*n*-3, 18:2*n*-6, 18:3*n*-3, 20:4*n*-6, 20:5*n*-3, 20:3*n*-6, 20:4*n*-3, 20:2 and 20:3*n*-3, indicating that the triacylglycerol mixture is comprised of at least five different compounds.

Cystophora xiphocarpa also yielded a series of eight polyoxygenated steroids (**94–101**), which includes three pairs of diastereomers, as well as a phaeophytin (**102**). Investigation of the stereochemistry of the isolated steroids included the derivatisation of compound **94** using phosgene to form a cyclic carbonate (**106**), molecular modelling and coupling constant (*J*) analysis of each compound. As a result, the stereochemistry of only one pair of diastereomers remains undefined. Unfortunately these steroids decomposed before anticancer bioassay data could be obtained. The biosynthesis of steroids is also discussed and a biosynthetic pathway of each of the steroids identified during this research is proposed.

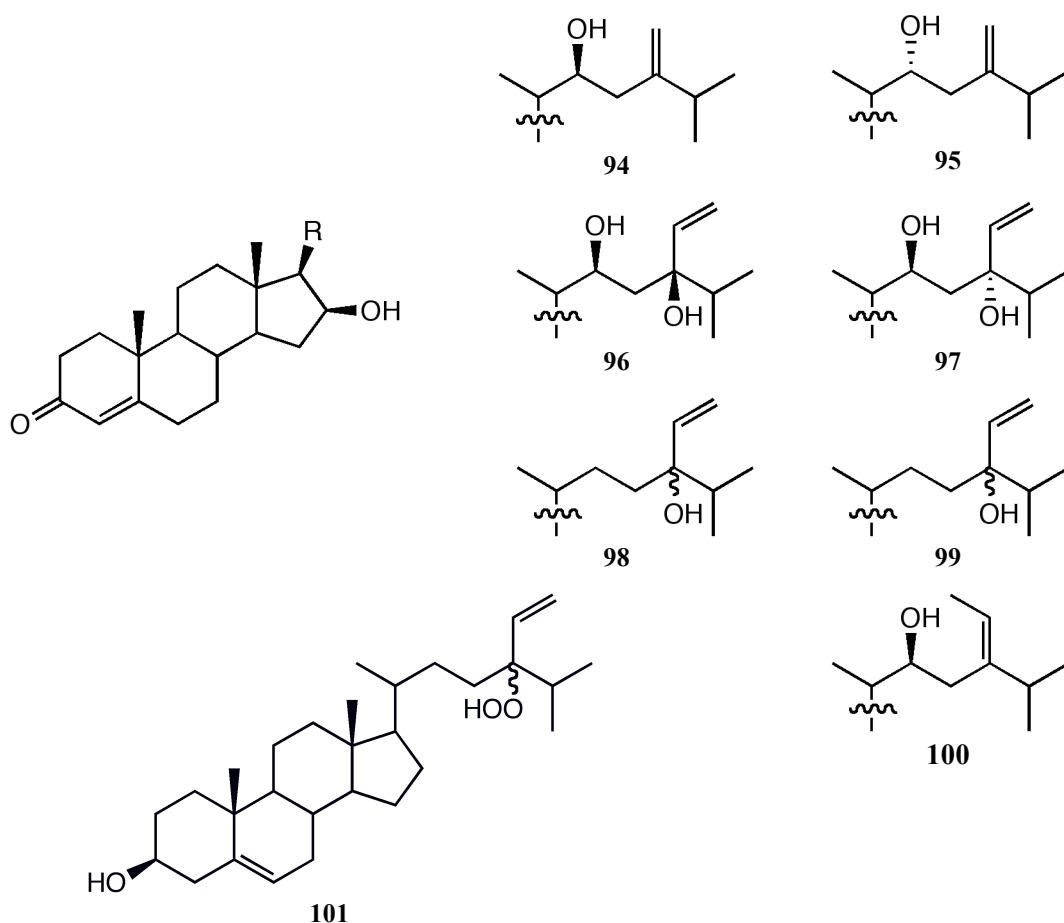


Table of Contents

1	Endocytosis and Disease	1
1.1.1	Clathrin-Dependent Endocytosis	2
1.1.2	Clathrin Mediated Endocytosis & Synaptic Vesicle Recycling	3
1.2	<i>Dynamin</i>	6
1.2.1	Tertiary Structure	7
1.2.2	Mode of Action	8
1.2.3	Other Processes Involving Dynamin	8
1.2.4	Synaptic Vesicle Recycling, Dynamin and Disease	12
1.2.5	Summary	16
1.2.6	Domains of dynamin	17
1.2.7	Targets	21
1.3	<i>Dynamin Assay</i>	21
1.4	<i>Current Dynamin Inhibitors</i>	22
1.5	<i>Chemical Space</i>	25
1.5.1	Synthetic Compounds	25
1.5.2	Natural Product Compounds	26
1.5.3	Natural Products versus Synthetic drugs	27
1.5.4	Conclusions	29
2	Natural Products	30
2.1	<i>Marine Natural Products</i>	32
2.2	<i>Drugs From Natural Products</i>	35
2.2.1	Dereplication	35
2.2.2	Mass Conservation	36
2.2.3	Limitations of Bioassay-Guided Drug Discovery	36
2.2.4	Artifacts	37
2.3	<i>Results</i>	38
2.3.1	Collection and Extraction	38
2.3.2	Crude Extract Screening	38

2.4	<i>Isolation of Eicosapentaenoic methyl ester</i>	44
2.4.1	Biological activity of fatty acids	48
2.4.2	Bioactivity of Compounds 15 and 16	49
2.5	<i>Isolation of Steroids from Psammoclema sp.</i>	51
2.5.1	Compounds from <i>Psammoclema</i> sp.	69
2.5.2	Sterols from the order <i>Poecilosclerida</i>	71
2.5.3	Conclusions	72
3	Chemotaxonomy of <i>Cystophora</i> sp.	74
3.1.1	Taxonomy	74
3.1.2	Chemotaxonomy	77
3.1.3	Chemotaxonomy of Phaeophyta (Brown algae)	78
3.1.4	The Genus, <i>Cystophora</i>	79
3.2	<i>Chemistry of Brown Algae of Cystophora sp.</i>	79
3.2.1	Phylogeny of <i>Cystophora</i>	87
3.2.2	Chemical investigation of two species of <i>Cystophora</i>	94
3.3	<i>Compounds from Cystophora torulosa</i>	96
3.3.1	Polyenes from <i>Cystophora torulosa</i>	97
3.3.2	Isoprenyl Chroman from <i>Cystophora torulosa</i>	99
3.3.3	Resorcinol from <i>Cystophora torulosa</i>	99
3.3.4	Fucosterol from <i>Cystophora torulosa</i>	100
3.3.5	Conclusions	100
3.4	<i>Compounds from Cystophora xiphocarpa</i>	102
3.4.1	Triacylglycerols from <i>Cystophora xiphocarpa</i>	103
3.4.2	Conclusions:	109
3.5	<i>Steroids from Cystophora xiphocarpa</i>	110
3.5.1	Isolation	110
3.5.2	Structure elucidation of 94	113
3.5.3	Structure Elucidation of Compound 95	119
3.5.4	Planar structures of steroid 94 and 95	122
3.5.5	Structure Elucidation of Compound 96	122

3.5.6	Structure Elucidation of Compound 97	125
3.5.7	Structure Elucidation of Compounds 98 and 99	130
3.5.8	Structure Elucidation of Compound 100	134
3.5.9	Another Steroid Compound 101	139
3.5.10	Steroids 94–99 Stereochemistry	141
3.5.11	Phaeophytin	142
3.6	<i>Stereochemistry of Steroids 94–99</i>	143
3.6.1	Stereochemistry of Compound 94	143
3.6.2	Structure of the Steroid Carbonate, Compound 106	144
3.6.3	Carbonate Reaction Minor Product, compound 107	147
3.6.4	Stereochemistry of Compound 106	151
3.6.5	Molecular Modelling	155
3.6.6	Stereochemistry at C-16 of Compounds 94–99	159
3.6.7	Determination of Stereochemistry at C-22 of the Remaining Steroids	160
3.6.8	Predicted Versus Actual Coupling Constants	162
3.6.9	Stereochemistry at C-22 of Compounds 94–97 and 100	163
3.6.10	Absolute Stereochemistry by Mosher’s Ester Analysis	166
3.6.11	Stereochemistry Summary	167
4	Biosynthesis of Steroids	169
4.1.2	Oxysterols and Oxidation	175
4.1.3	Proposed Biosynthesis of Isolated Steroids	177
4.1.4	Marine Steroids	181
4.1.5	Steroids as Chemotaxonomic Markers	181
4.1.6	Conclusions	185
5	Experimental	186
5.1.1	General	186
5.1.2	Animal and Plant Material	188
5.1.3	Biological Screening	189
5.1.4	Isolation of Steroids from a <i>Psammoclema</i> sp.	190
5.1.5	Isolation of Polyunsaturated Fatty Acid Esters from a sponge	193

5.1.6	Isolation of Compounds from <i>Cystophora torulosa</i>	195
5.1.7	Isolation of Triacylglycerols from <i>Cystophora xiphocarpa</i>	199
5.1.8	Isolation of Steroid Series from <i>Cystophora xiphocarpa</i>	201
5.1.9	Derivatisation of Compound 94	209
5.1.10	References	214

Table of Tables

Table 1. NMR Spectroscopic Data for Compound 17 with Supporting 1D and 2D NMR Correlation Information	56
Table 2: Comparison of ^{13}C NMR chemical shifts for 24-ethyl steroids.	58
Table 3: Comparison of chemical shifts for -22-ene-24-methyl- steroids	62
Table 4: ^{13}C NMR Spectroscopic Data (75 MHz, CDCl_3) for Compounds 17–20 and 22	65
Table 5: ^1H NMR Spectroscopic Data (CDCl_3) for Compounds 17–20 and 22	66
Table 6: Growth inhibition (GI) response determined in HT29 (human colorectal), MCF-7 (human breast), A2780 (human ovarian) and DU145 (human prostate) cancer cell lines by the MTT cytotoxicity assay after 72 h continuous exposure to the compounds.	67
Table 7: Proton NMR data of compound 93 .	107
Table 8: GC-MS analysis of the methyl ester mixture of fatty acids transesterified from a triacylglycerol mixture from <i>C. xiphocarpa</i> .	109
Table 9: Comparison of ^{13}C and ^1H spectroscopic data of compound 94 with selected published data of compounds 102 and 103 ^{229, 230}	117
Table 10: ^1H and ^{13}C NMR data of compound 94 with supporting 2D correlation information	118
Table 11: ^1H and ^{13}C NMR Spectroscopic Data of Compound 95 with supporting 2D correlation information	121
Table 12: ^1H and ^{13}C NMR Spectroscopic Data of Compound 96	126
Table 13: ^1H and ^{13}C NMR Spectroscopic Data of Compound 97	129
Table 14: ^1H and ^{13}C NMR data of compound 100 with supporting 2D correlation information	138
Table 15: Comparison of ^1H NMR data of the <i>C. xiphocarpa</i> steroid, compound 101 , to literature values reported by Sheu <i>et al.</i> ²³²	141
Table 16: Comparison of the NMR spectroscopic data of the compound 106 in CDCl_3 and C_6D_6	149

Table 17: Comparison of Compound 106 Modelling Data	161
Table 18: <i>C. xiphocarpa</i> steroids and their assigned stereocenters	167
Table 19: Pulse programs used during NMR experiments	186
Table 20: ¹³ C NMR Spectroscopic Data (75 MHz, CDCl ₃) for the pure steroids (94–97 , 100 and 106) isolated from <i>C. xiphocarpa</i>	205
Table 21: ¹ H NMR Spectroscopic Data (300 MHz, CDCl ₃) for the pure steroids (94–97 , 100 and 106) isolated from <i>C. xiphocarpa</i>	206
Table 22: ¹ H and ¹³ C NMR data of compound 94 -diacetate	210

Table of Figures

Figure 1: Formation of an endocytic vesicle	2
Figure 2: Internalisation of a clathrin-coated vesicle	3
Figure 3: Vesicle collapse versus kiss-and-run	4
Figure 4: A: A Deeply invaginated collar pit; B: Budding vesicles not excised from the cell membrane	5
Figure 5: Dynamin family members and their numerous cellular processes	7
Figure 6: Dynamins mode of action	8
Figure 7: Dynamin in centrosome separation	9
Figure 8: Mutations of dynamin-like proteins and known associated diseases	14
Figure 9: Schematic representation of the five domains of dynamin-I	17
Figure 10: Schematic representation of the domain structure of OPA1 compared to dynamin	18
Figure 11: Schematic structure of synamin showing GED and middle domains as a connector between the GTPase and PH domains	20
Figure 12: Principal component analysis of three compound databases	29
Figure 13: Sources of new chemical entities published between January 1981 and June 2006 (<i>N</i> = 974)	30
Figure 14: The proportion of natural products in anticancer drugs released between the 1940's and June 2006 (<i>N</i> = 175)	31
Figure 15: Percentage of biologically active 'positive hits' of compounds isolated from various sources	33
Figure 16: Early dynamin-I bioassay results from screening of crude extracts 37A, 47N and 47G	39

Figure 17:	Dynamamin-I bioassay results of the crude sponge extracts 53G, 41G, 39G and 48M	40
Figure 18:	Dynamamin-I bioassay results of the sponge fractions 53D, 53E and 53F	43
Figure 19:	Common α - and ω -mass fragments associated with <i>n</i> -3 and <i>n</i> -6 methylene interrupted polyunsaturated C-20 fatty esters	46
Figure 20:	Key features of the CG-MS spectrum of compound 15 including the α -fragment at $m/z = 180$	47
Figure 21:	The marine sponge, <i>Psammoclema</i> sp., collected at The Pipeline, Nelson Bay	51
Figure 22:	Key 2D NMR spectroscopic correlations of compound 17	53
Figure 23:	Key NOE observations of compound 17	55
Figure 24:	DQF-COSY correlations (bold bonds) for the steroidal side chains of compounds 18–20	64
Figure 25:	Possible phylogenetic relationships of the <i>Cystophoras</i> based on morphology	88
Figure 26:	Proposed chemical phylogeny of those species of <i>Cystophora</i> for which chemical data is available	92
Figure 27:	Dendrogram of the phylogeny of 14 <i>Cystophora</i> species based on their ITS-2 sequences	94
Figure 28:	<i>Cystophora torulosa</i> collected from Cook Straight, New Zealand	96
Figure 29:	<i>Cystophora xiphocarpa</i> collected from Spikey Beach, Tasmania, Australia	102
Figure 30:	TLC of speedy column fractions visualized using <i>p</i> -anisaldehyde	103
Figure 31:	Proton NMR spectrum of triacylglycerol mixture in CDCl ₃ between 0–7.5 ppm	105
Figure 32:	Example of a mixed triacylglycerol	106
Figure 33:	GC-MS chromatogram of the triacylglycerol acyl methyl esters	109
Figure 34:	The structure of 94 showing key DQF-COSY and gHMBC correlations	116
Figure 35:	Key COSY-45 and gHMBC correlations of compound 96	120
Figure 36:	The planar carbon skeleton of compounds 95 and 96 is shown with dots to represent the differences in ¹³ C NMR data between the two steroids	122
Figure 37:	Key COSY-45 and gHMBC correlations of compound 97	125
Figure 38:	Key COSY-45 and gHMBC correlations of compound 98	128
Figure 39:	Comparison of the ¹ H NMR spectra of compound 97 (above) and the M1/M2 mixture (below) between 3.5 and 6.0 ppm	132
Figure 40:	Key COSY-45 and gHMBC correlations of the mixture of compounds 99 and 100	134
Figure 41:	Key COSY-45 and gHMBC correlations of compound 101	136
Figure 42:	Key NOE correlations of compound 101	137
Figure 43:	Structure of compound 108 determined by spectroscopic techniques	147

Figure 44:	Proton NMR spectrum of compound 108	151
Figure 45:	NOESY spectrum of compound 108 with a mixing time of 800 ms	152
Figure 46:	(I) Key NOESY correlations of compound 108 . (II) Key NOESY correlations observed by Achembach <i>et al.</i>	155
Figure 47:	Molecular modelling structure of the D- and E-rings of the lowest energy configuration of the 16 <i>S</i> ,22 <i>R</i> diastereomer of compound 108	157
Figure 48:	The D- and E-rings and orientation of the steroidal side chain of compound 108 in the compounds two lowest conformations are shown	158
Figure 49:	Proton NMR spectra showing the comparison of the oxymethine protons of compounds 95–100	159
Figure 50:	Comparison of the ¹ H NMR signals of H-22 of steroids 95 (above) and 96 (below)	164
Figure 51:	Molecular modelling of the chiral centre at C-24, 24 <i>S</i> (left) and 24 <i>R</i> (right) to determine the stereochemistry of 97 and 98	165
Figure 52:	Biosynthetic origins of steroids comparing animals, fungi and higher plants	169
Figure 53:	Standard steroid nucleus showing ring naming and numbering	170
Figure 54:	Typical steroid nuclei with differing ring junction stereochemistry	171
Figure 55:	Example of steroid nucleus modification	173
Figure 56:	Alkylation of a steroid side chain by SAM	174
Figure 57:	The formation of 24-hydroperoxy-24-vinyl steroidal side chains via a per-epoxide (above) or via a concerted mechanism (below)	177
Figure 58:	Possible biosynthetic route for the steroid nuclei isolated from the marine sponge <i>Psammoclema</i> sp.	178
Figure 59:	Possible biosynthetic route for the steroid tails isolated from the marine sponge <i>Psammocelmma</i> sp.	179
Figure 60:	Possible biosynthetic <i>C. xiphocarpa</i> steroidal side chain modifications starting with a cycloartenol side chain	180
Figure 61:	Possible biosynthetic route of the steroid nucleus of compounds 95–101	181
Figure 62:	Flow diagram of the separation procedures used to purify steroids from a marine sponge of a <i>Psammoclema</i> sp.	192
Figure 63:	Flow diagram showing the isolation of compounds from <i>C. torulosa</i>	196
Figure 64:	Flow diagram of the separation procedures used to purify compounds from <i>C. xiphocarpa</i>	208
Figure 65:	Reaction of compound 95 to form 108	212
Figure 66:	TLC of the reaction mixture of compound 95 and COCl ₂ visualised using phosphomolybdic acid dip	212
